CHARACTERISTICS OF MAGNETIC SOURCES IN THE REGION OF THE LUNAR SOUTH POLE - AITKEN BASIN. L.C. Newman and D. Ravat, Earth and Environment Sciences, University of Kentucky, Lexington, KY 40506, USA, leah.newman@uky.edu, dhananjay.ravat@uky.edu

Introduction. Satellite missions carrying magnetometers to the Moon (Lunar Prospector and SELENE) have shown stronger magnetic anomalies in the South Pole–Aitken basin (hereafter referred to as SPA) in comparison to other regions. The SPA magnetic anomalies have cross-cutting features and have been disparately interpreted as either magnetization due to electric fields from antipodal impacts [1], surficial features due to iron-rich impact ejecta [2], or basaltic dike swarms and intrusions magnetized during the dynamo episode [3]. The first two interpretations require different magnetic source geometries than the latter one. Using a new pass-by-pass correlation technique, which takes into account the varying altitude of the data, we select the cleanest low-altitude (≤50km) orbital data segments over SPA from the SELENE (Kaguya) mission to improve anomaly resolution. We then create a 3 component equivalent source crustal dipole representation to altitude normalize the field over SPA and surrounding regions (with spatial resolution of ~20km wavelength) and use it to constrain and interpret the geometry and locations of key sources. New and advanced spectral source depth determination techniques suggest that there is a regional magnetic layer near the surface with varying thickness of 16-26 km. The layer also exists in the region lacking strong magnetic variations. Euler Deconvolution results suggest that there are both dike-like and sill-like sources penetrating through this layer. Since there are no detectable "edges" to the regional magnetized layer in the global field, the results imply that the Moon has a magnetized outer shell formed under the influence of an internal dipolar core field [4].

Data Selection. SELENE magnetic field data were split into ascending and descending passes, internal and external fields related dipole models were removed [3] and quadratic detrending was performed [1]. Along pass equivalent source inversion was used to isolate consistent signal in each of the components from neighboring passes (a new technique, procedure in Figure 1 caption). Many of the descending passes were contaminated by external fields and only clean descending passes in the region of gaps in ascending passes were used to fill-in for the regional equivalent source inversion and altitude normalization.

Altitude Normalization of the Regional Data Set. Equivalent source inversion [5, 6] was used with dipoles at 2° polar tessellate equal area locations at the depth of 20km under the SPA and surrounding regions and the resulting fields were computed at 30 km altitude (see Figure 2 for details).

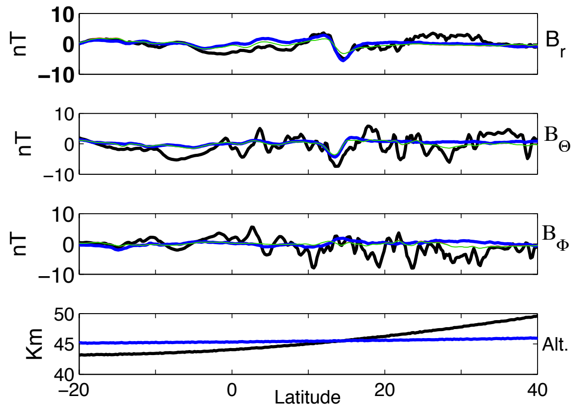

Figure 1. The procedure to differentiate crustal signal from the external field effects. Comparison of pass 4715 (black) and pass 5060 (blue) in the same longitudinal bin with different altitudes. Panels from top to bottom show B_r, B_θ, B_Φ and altitude. Equivalent sources are laid at the Moon's surface between the two profiles. Fields computed from the equivalent sources for both profile locations follow the observations in pass 5060 (in places one can see the computed field in green line slightly away from the blue line, and the computed field from pass 4715 are completely hidden by the green line). This suggests that the observations in pass 4715 (which are not fit well by the fields from the equivalent sources) must be contaminated by external fields. In addition, other neighboring passes (within 1° longitude) are used to cross-check this inference. The southernmost anomaly features seen in B_r are consistent between the two observed as well as computed profiles and so they indicate the crustal origin of the fields; this portion of the pass is retained.

Spectral approach to infer regional depth structure. In order to constrain the magnetic source geometry we used a modified spectral method of Salem et al. [7] where slopes and peaks of spectra are used to infer the depths to top, bottom, and the fractal parameter of the field (see results in Table 1).

Table 1. Spectral depth results with respect to the Lunar radius of 1738km. Negative depths are in the regions of high topography.

Latitude	Longitude	Window size (km)	Depth to top (km)	Depth to bottom (km)
-25°	160°	500	-3 - -4	17 - 18
-25°	170°	1000	0 - 2	16
-25°	170°	500	0	16 - 26
-25°	180°	500	-2 - -2	16 - 24
0°	195°	500	2	16

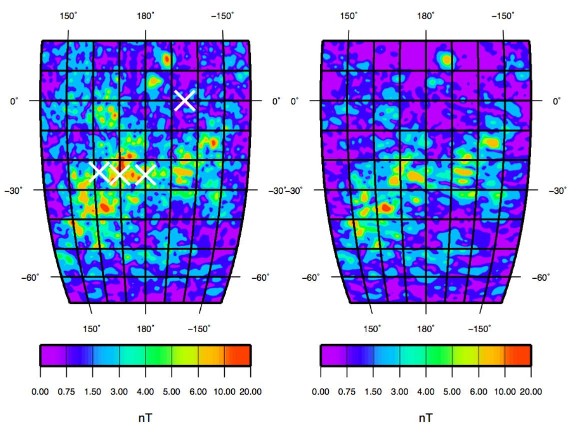

Figure 2. Total fields calculated at 30km altitude from our SELENE data selection and equivalent source altitude normalization (left) and Purucker et al.'s spherical harmonic model of fields from Lunar Prospector [8] (right). Most features are consistent between the two maps; however, our SELENE total intensity field has higher spatial resolution (λ~20km) apparent from the detail in the map (left) and spectral analysis. The LP spherical harmonic degree 178 model has the shortest RMS wavelength of about ~50km. Our SELENE total intensity field also has stronger and coherent signal. White Xs indicate centers of windows used for depth determination in Table 1.

Euler Deconvolution in determining source geometry. We used Euler Deconvolution with a structural index of 1 (which, based on the continuity of the source locations, can be used to identify both dike-like and sill-like sources) [9]. Selected solution concentrations from a 50x50km moving Euler window show the presence of both sill-like (oval-shaped solution distribution) and dike-like sources (linear) (Figure 3).

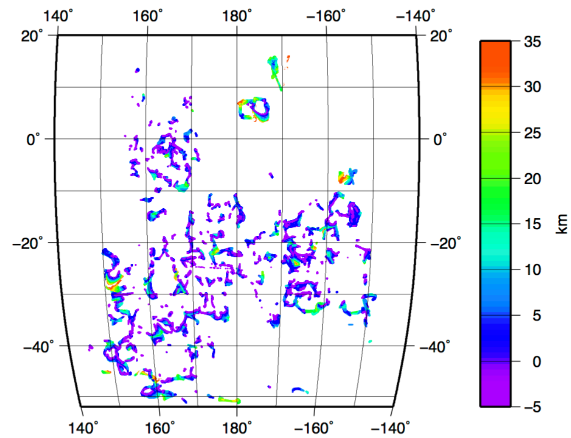

Figure 3. Euler solutions in the region of interest, displaying depths to the top of magnetic sources. Sources with negative depths indicate near-surface locations. Due to the nature of the spread of solutions in the Euler Method, we generally interpret the shallowest parts of the trends. The circular nature of the feature centered at 7°N, 183°E is in direct agreement to the visible anomaly seen in both the SELENE and LP maps (Figure 2). Euler solution linear trends (dikes) are in several directions and oval-shaped solution features indicate some of the sill-like ponds at various crustal depths.

More work is underway to validate these preliminary results by performing additional analyses, improving the map resolution by adding Lunar Prospector data, and extending analyses to neighboring regions.

References

[1]Hood, L. L. et al. (2013). *JGR 118*, 1265-1284.
[2]Wieczorek, M. A. et al. (2012). *Science 335*, 1212-1215.
[3] Purucker, M. E. et al. (2012). *JGR 117*, E05001. 237, 262 -277.
[4] Runcorn, S.K. (1975). *PEPI 10,* 327-335
[5] Dampney C. N. G. (1969) *Geophysics 45,* 39 – 53.
[6] Langlais, B. et al. (2004). *JGR 108,* E02008.
[7] Salem, A. et al. (2014) *Tectonophysics 624-625,* 75-86.
[8] Purucker, M. E. and Nicholas, J.B. (2010). *JGR 115*, E12007.
[9] Ravat, D. et al. (2002). *J Geodynamics 33, 131-142.*